Supplementary Materials

Abnormal dynamic ventilation function of COVID-19 survivors detected by pulmonary free-breathing proton MRI

This file includes two parts:

1. Supplementary methods (detailed description of mPREFUL)

2. Supplementary results (Fig. S1, Fig. S2, Fig. S3)

    Comparison between dynamic and static ventilation (Fig. S1)

    N-phase ventilation results (Fig. S2)

    Comparison between FV and lung volumes (Fig. S3)

Supplementary methods

The general framework of the proposed mPREFUL method included three major procedures: 1) time-series signal construction, 2) full respiratory cycle (FRC) reconstruction, and 3) dynamic ventilation maps generation, as shown in Fig. 1.

In the first step, the time-series signal was constructed. In original PREFUL [1], a region of interest (ROI) in unilateral lung was manually selected, and the mean [1]H-density of that ROI was used to construct the time-series signal. Nevertheless, the residual regional lesions (e.g., ground glass opacities or consolidation) may exist in COVID-19 survivors [2]. Considering the residual COVID-19 lesions could not be displayed so clearly in ^{1}H MRI images [3], that ROI might include potential lesions in some survivors or not in others, and then affected the group results. The different locations of that ROI in a same survivor could also affect the final result of that survivor [4]. Besides, the affection of contralateral lung in the time-series signal was also not considered.

Thus, in mPREFUL, we used the mean [1]H-density of whole lung to construct the time-series signal, which could be automatically obtained after lung segmentation. Previous studies have demonstrated the [1]H-density of lungs could be used to reflect the lung volumes (i.e., respiratory phase) [5, 6]. For a given image x in the registered time-series ^{1}H MRI, the mean [1]H-density of whole lung (denoted as ρ_x) was calculated, which represented the respiratory phase (denoted as $\alpha_x \in [0, 2\pi]$) of that image. After low-pass filtering and removing outliers, these dynamic [1]H-density signal was used as the time-series signal.

In the second step, the FRC was reconstructed. In original PREFUL, the respiratory frequency (RF) of the time-series signal for all the subjects was set as a same arbitrary value (e.g., 0.3 Hz). This may obscure individual differences. While in mPREFUL, the actual RF of each subject was obtained by

using the Fourier decomposition (FD) method [6], and the corresponding respiratory cycle time (denoted as T_{FRC}) of each subject could be calculated,

$$T_{FRC} = 1 / RF \tag{1}$$

Then according to the slopes of the time-series signal, the time-series ^{1}H MRI images were divided into expiration phase (exp-phase) or inspiration phase (insp-phase). After that, the ^{1}H MRI images in the exp-phase or insp-phase were sorted based on the their ρ_x values to restore its real order (not the acquisition order) in FRC. Via normalization ([-1,1]) of ρ_x, the relationship between their ρ_x values and actual respiratory phase (α_x) could be considered as cosine function [1, 6],

$$\alpha_x = \begin{cases} \cos^{-1}(-\rho_x), & \text{if } \alpha_x \in exp\text{-}phase \\ 2\pi - \cos^{-1}(-\rho_x), & \text{if } \alpha_x \in insp\text{-}phase \end{cases} \tag{2}$$

Combining with the calculated T_{FRC}, the α_x could be further transformed to the actual respiratory time (denoted as $t_x \in [0, T_{FRC}]$),

$$t_x = (\alpha_x / 2\pi) * T_{FRC} \tag{3}$$

In the third step, the dynamic ventilation maps were generated. The change of air content in pulmonary voxel between two respiratory phase [e.g., end-inspiration (end-insp) and end-expiration (end-exp)] would cause the change in [1]H-density [7]. Then the [1]H-density difference map [7] and relative difference map [8] between two lung volumes could be used to assess regional lung ventilation function. Thus, the dynamic [1]H-density difference maps and dynamic [1]H-density relative difference maps between each time point (t_x) ^{1}H MRI image and the end-exp ^{1}H MRI image in the FRC could be used to represent the dynamic ventilation maps [denoted as V(t_x) maps] and dynamic fractional ventilation maps [denoted as FV(t_x) maps], respectively. The V(t_x) maps and FV(t_x) maps were,

$$V(t_x) = {}^1H(end\text{-}exp) - {}^1H(t_x)$$
$$FV(t_x) = [{}^1H(end\text{-}exp) - {}^1H(t_x)] / {}^1H(end\text{-}exp) \tag{4}$$

Thus, in mPREFUL, the dynamic ventilation maps could be automatically generated without manual intervention, and the contribution of contralateral lung in the dynamic ventilating imaging was

also considered. Besides, the actual respiratory frequency and respiratory cycle time of each subject

were calculated. Correspondingly, the dynamic ventilation parameters of the subjects were assessed

based on their real respiratory time.

Supplementary results

Comparison between dynamic and static ventilation

Figure S1 showed the ^{1}H MRI images, Fourier decomposition ventilation (FD-V) maps, $V_{100\%}$ maps, and $FV_{100\%}$ maps of a healthy volunteer (male, 46 years old), a mild COVID-19 survivor (female, 29 years old), and a severe COVID-19 survivor (male, 31 years old). The FD-V map was used as the static ventilation map. The $V_{100\%}$ map and $FV_{100\%}$ map were used as the dynamic ventilation maps. In the FD-V maps, it was found that the distribution of signal intensities in the healthy volunteer was similar with those in the mild and severe survivors in visual. As for the $V_{100\%}$ maps and $FV_{100\%}$ maps, lots of hyperintense signal areas (i.e., high ventilation areas, indicated by red color in $V_{100\%}$ maps and $FV_{100\%}$ maps) existed both in the mild and severe survivors. These results indicated that dynamic ventilation maps were more sensitive to detect regional ventilation abnormity in COVID-19 survivors compared with static ventilation maps.
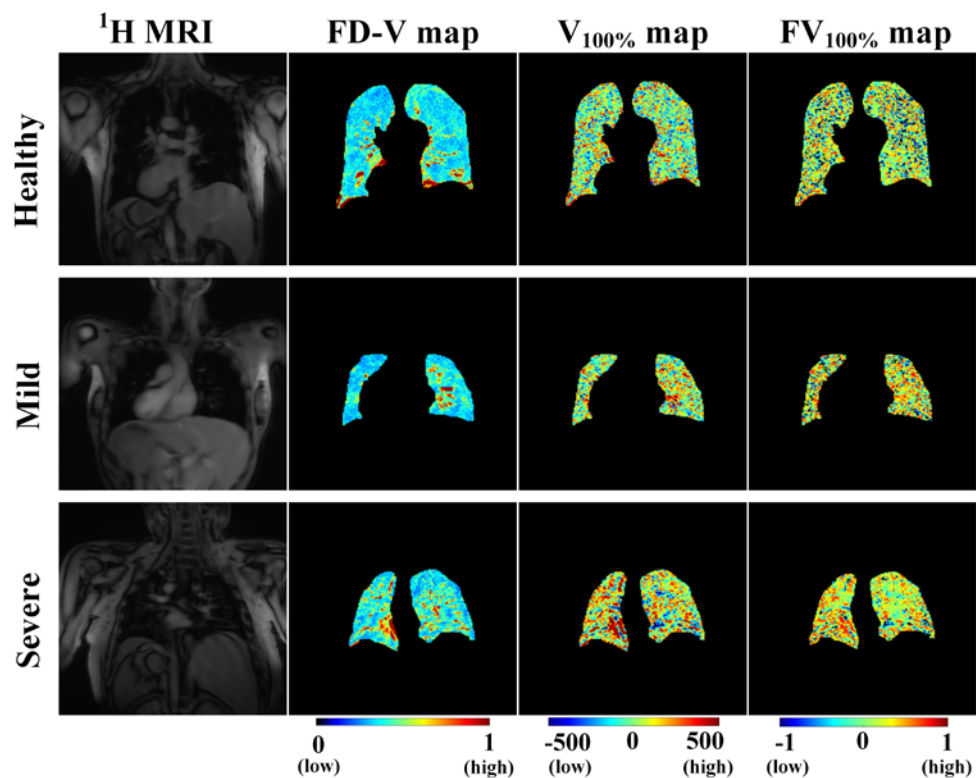
Fig. S1 The ^{1}H MRI images, FD-V maps, $V_{100\%}$ maps, and $FV_{100\%}$ maps of a healthy volunteer (male,

46 years old), a mild COVID-19 survivor (female, 29 years old), and a severe COVID-19 survivor (male, 31 years old). The FD-V map was used as the static ventilation map. The $V_{100\%}$ map and $FV_{100\%}$ map were used as the dynamic ventilation maps. The hyperintense signal areas (red color areas) of ventilation maps indicated high ventilation areas

N-Phase ventilation results

The $V_{100\%}$ map generated from the end-exp and end-insp ^1H MRI images in full respiratory cycle (FRC) suffers from the fact that some regions of the lung may reach their maximum and minimum volumes at different respiratory phases than the total lung volume. Thus, in this work, the N-Phase ventilation method [9] was used to adjust the $V_{100\%}$ maps. In details, the sorted 189 time-series ^1H MRI images were firstly resampled to 10 respiratory phase ^1H MRI images. Then the 10 ventilation values of a pixel in lungs were calculated. After that, the max ventilation value and min ventilation value were extracted to reconstruct the real ventilation value of that pixel.

Figure S2 showed the adjusted $V_{100\%}$ maps of the 3 representative subjects in Fig. 2. Similar with the original $V_{100\%}$ maps, the signal intensities in the adjusted $V_{100\%}$ map of the healthy volunteer were homogeneous, while lots of hyperintense signal areas existed in the adjusted $V_{100\%}$ maps of the COVID-19 survivors. Quantitatively, the mean value of adjusted $V_{100\%}$ map in COVID-19 group was significantly higher than that in healthy group (66.2 ± 19.8 vs 40.0 ± 10.3; $P < 0.001$). Besides, the ratio of the out-of-phase ventilation pixels (i.e., the pixels that the adjusted ventilation values were higher than the original ventilation values) and the total lung pixels in the COVID-19 group was also significantly higher than that in healthy group (8.9% ± 1.2% vs 7.7% ± 0.7%; $P = 0.003$). N-Phase ventilation results revealed the differences between the COVID-19 and healthy groups.

The N-Phase ventilation method has been demonstrated it could detect more accurate ventilation values between the end-exp and end-insp images [9]. Howbeit, the original N-Phase ventilation method was proposed based on the 4D-CT images using the Jacobian ventilation model [10]. In this study, the ventilation maps were generated based on free-breathing ^{1}H MRI images using the density difference ventilation model [7, 8]. In the future, more efforts are needed to apply the N-Phase method in ^{1}H MRI ventilation imaging.
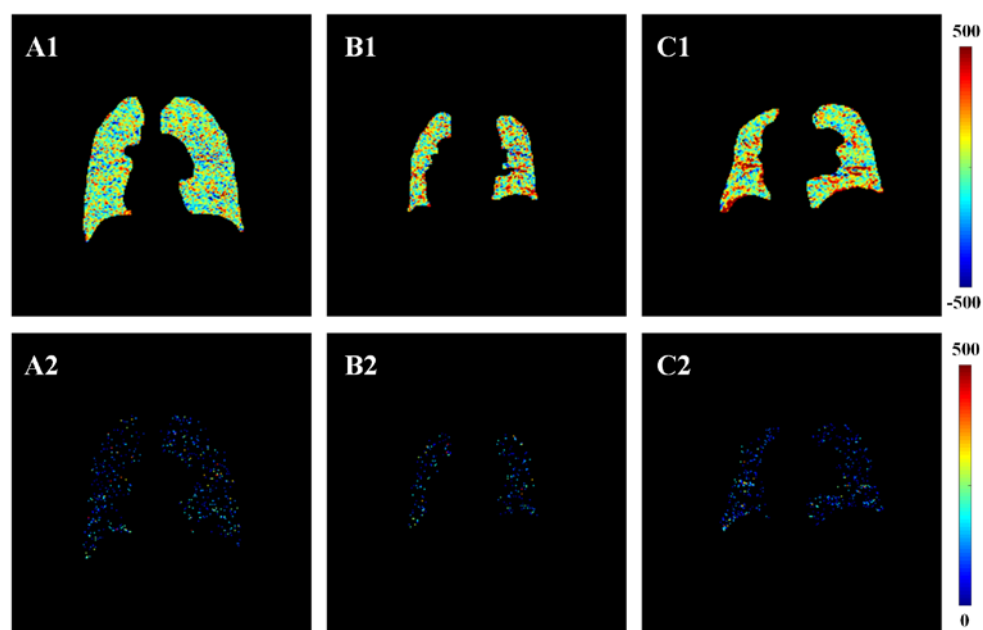
Fig. S2 The N-Phase ventilation results of the 3 representative subjects in the Fig. 2. A1-C1, The adjusted $V_{100\%}$ maps of the healthy volunteer (male, 31 years old), mild COVID-19 survivor (female, 47 years old), and severe COVID-19 survivor. A2-C2: The difference maps between the original $V_{100\%}$ maps and the adjusted $V_{100\%}$ maps

Comparison between FV and lung volumes

Fractional ventilation (FV) is a measurement of ventilation per unit volume. To investigate the differences in FV between the healthy volunteers and COVID-19 survivors are due to the changes in

functional residual capacity or due to the changes in tidal volume, the end-insp lung volume, end-exp

lung volume (i.e., functional residual capacity), and expanded lung volume (end-insp lung volume

minus end-exp lung volume, i.e., tidal volume) were extracted based on the lung segmentation of the

free-breathing ^{1}H MRI images (the details were described in the subsection **Validation of mPREFUL**

of **Materials and methods,** as shown in Fig. 6a).

Then the FV values (including the measured FV_{Global} values and the calculated mean FV values of

$FV_{100\%}$ maps) were compared with the lung volumes for all subjects. Fig. S3 showed the group analysis

of the lung volumes, the Pearson correlation between the FV_{Global} values and the lung volumes, and the

Pearson correlation between the mean FV values of $FV_{100\%}$ maps and the lung volumes. It could be

seen that, excepting expanded volume (tidal volume) ($P = 0.013$), there were no significant differences

between the COVID-19 group and healthy group regarding the lung volumes. The correlation between

expanded volume (tidal volume) and FV ($r = 0.65$; $P < 0.001$) was also stronger than the correlation

between end-exp lung volume (functional residual capacity) and FV ($r = -0.51$; $P = 0.003$). The results

showed the differences in FV between the healthy and COVID-19 groups were more correlated with

the changes in breathing volumes.
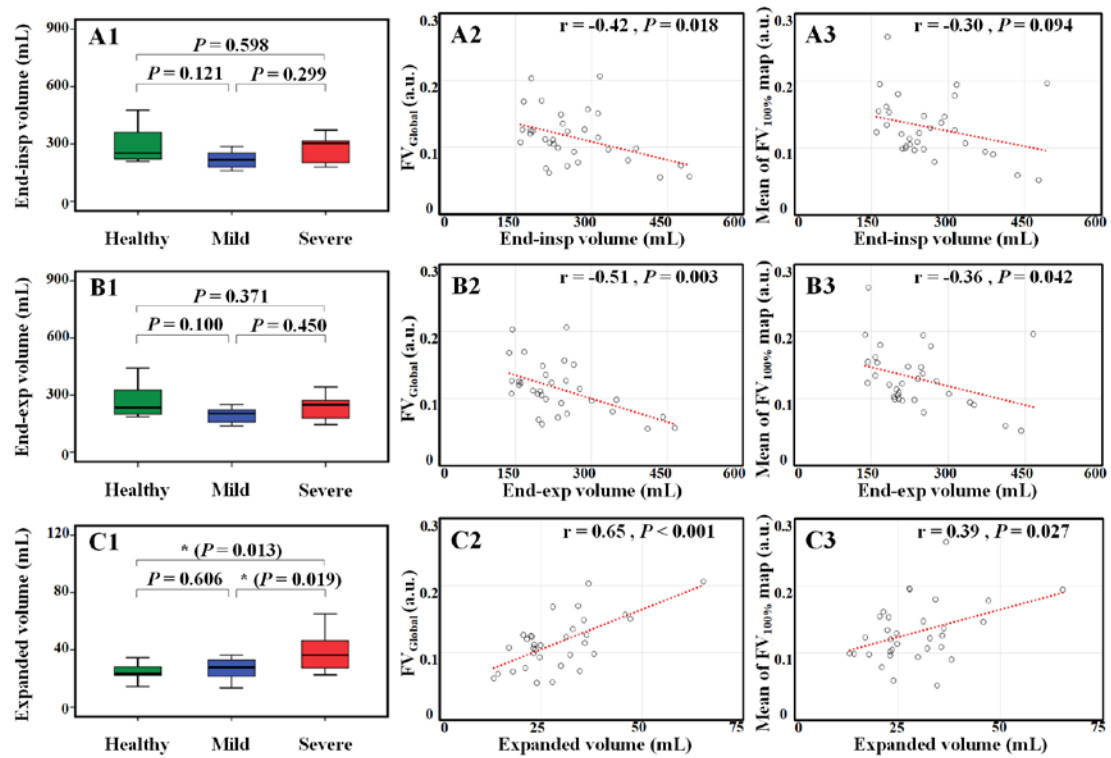
Fig. S3 The comparison between FV and lung volumes for all subjects. A1-C1, The group analysis (healthy, mild COVID-19, and severe COVID-19 groups) of the lung volumes [end-insp lung volume, end-exp lung volume (functional residual capacity), and expanded volume (tidal volume)]. A2-C2, The Pearson correlation between the measured FV_{Global} values and the lung volumes. A3-C3, The Pearson correlation between the calculated mean FV values of $FV_{100\%}$ maps and the lung volumes. The symbol * meant $P < 0.05$

References

1. Voskrebenzev A, Gutberlet M, Klimes F, et al (2018) Feasibility of quantitative regional ventilation and perfusion mapping with phase-resolved functional lung (PREFUL) MRI in healthy volunteers and COPD, CTEPH, and CF patients. Magn Reson Med 79(4):2306-2314

2. Huang Y, Tan C, Wu J, et al (2020) Impact of coronavirus disease 2019 on pulmonary function in early convalescence phase. Resp Res 21(1):163

3. Yang S, Zhang Y, Shen J, et al (2020) Clinical potential of UTE-MRI for assessing COVID-19: patient- and lesion-based comparative analysis. J Magn Reson Imaging 52(2):397-406

4. Pöhler G H, Klimeš F, Behrendt L, et al (2021) Repeatability of phase-resolved functional lung (PREFUL)-MRI ventilation and perfusion parameters in healthy subjects and COPD patients. J Magn Reson Imaging 53:915-927

5. Bankier A A, O'Donnell C R, Mai V M, et al (2004) Impact of lung volume on MR signal intensity changes of the lung parenchyma. J Magn Reson Imaging 20(6):961-966

6. Bauman G, Puderbach M, Deimling M, et al (2009) Non-contrast-enhanced perfusion and ventilation assessment of the human lung by means of Fourier decomposition in proton MRI. Magn Reson Med 62(3):656-664

7. Pennati F, Quirk JD, Yablonskiy DA, Castro M, Aliverti A, Woods JC (2014) Assessment of regional lung function with multivolume ^{1}H MR imaging in health and obstructive lung disease: comparison with ^{3}He MR imaging. Radiology 273(2):580-590

8. Zapke M, Topf H, Zenker M, et al (2006) Magnetic resonance lung function – a breakthrough for lung imaging and functional assessment? A phantom study and clinical trial. Resp Res 7(1):106

9. Shao W, Patton T J, Gerard S E, et al (2019) N-phase local expansion ratio for characterizing

out-of-phase lung ventilation. IEEE T Med Imaging 39(6):2025-2034

10. Kipritidis J, Tahir B A, Cazoulat G, et al (2019) The VAMPIRE challenge: a multi-institutional

validation study of CT ventilation imaging. Med Phys 46(3):1198-1217